Int. J. Solids Structures, 1967, Vol. 3, pp. 951 to 966. Pergamon Press Ltd. Printed in Great Britain

NUMERICAL SOLUTION OF THE PROBLEM OF IMPACT OF A RIGID SPHERE ONTO A LINEAR VISCOELASTIC HALF-SPACE AND COMPARISON WITH EXPERIMENT

HARRY H. CALVIT*

Brown University, Providence, R.I.

Abstract—The pair of coupled nonlinear integro-differential equations which describe the impact of a rigid sphere onto a viscoelastic half-space are solved numerically. Using data obtained from free torsional vibration experiments, the rebound of a steel ball from a block of polymer is predicted for various temperatures. These results are compared with rebound experiments performed on the same material. The viscoelastic solution is also compared with elastic solutions and an approximate solution. Some conclusions are drawn on using the rebound method as a means of dynamic testing.

INTRODUCTION

THE contact problem of a spherical indenter and a half-space represents a special set of problems in the linear theory of viscoelasticity, that is, the mixed boundary value problem with time dependent boundaries. This problem is special in that solution through the appeal to the similarity between the transformed viscoelastic equations and the equations of elasticity breaks down due to the dependence of the boundary conditions on time. (However this does not preclude the use of transform methods altogether as shown by Ting [1].)

The first attempt to extend the Hertz solution for the elastic case to the linear viscoelastic case appears to be due to Pao [2]. Pao assumed that the difference in the contact area between the elastic solution and the viscoelastic solution was negligible (this assumption will be discussed later). He also assumed that the viscoelastic material was elastic in bulk compression. Under these assumptions he was able to obtain a single integro-differential equation which he solved numerically by assuming that the material had a finite number of relaxation or retardation times.

Lee and Radok [3] presented a solution to the problem by replacing the elastic constants in the solution to the associated elastic problem by viscoelastic functions. They then showed that the solution satisfied the necessary boundary conditions. However, they discovered that the solution for the penetration $\alpha(t)$ was only valid for $\alpha(t)$ nondecreasing.

Hunter [4] later produced the first "general" solution which was valid for the case where $\alpha(t)$ attained a single maximum.

Hunter's results were obtained by a generalization of the Boussinesq solution and entailed a solution of a pair of dual integral equations which arise frequently in mixed boundary value problems of this type. In obtaining the equations that will be presented later, he also assumed that the behavior of the material was identical in shear and in dilatation, thus giving a Poisson's ratio independent of time. Using a more direct approach,

* Now at: The University of Texas, Austin, Texas.

Graham [5] reproduced Hunter's results as well as solutions for other geometries. He used the generalized Papkovich Neuber stress function as a basis for his analysis.

Recently Ting [1] has shown that a generalized transform approach can also be used successfully to obtain the solution to the contact problem. By assuming an alternative boundary condition and applying the transform method, the problem can be solved formally in terms of the unknown boundary condition which is then determined. Using this method a solution to the contact problem with more than one maximum in the penetration was obtained. Also in some cases Ting has shown that simpler integro-differential equations are obtained through this approach.

INTEGRO-DIFFERENTIAL AND FINITE DIFFERENCE EQUATIONS

From the point of view of comparison with experiment, the solution of interest is the one which produces $\alpha(t)$ and $r_1(t)$, the penetration and radius of contact, respectively, since it is from these variables that one obtains the rebound height and the time that the sphere is in contact with the half-space.

The solution obtained by Hunter is in the form of a single integro-differential equation for monotone increasing penetration and a pair of coupled nonlinear integro-differential equations for the withdrawal.

Since the equations have been obtained in several ways by different authors, they will not be derived here.

If a ball of mass M and radius R is dropped onto a viscoelastic half-space whose mechanical properties are given by $\mu(t)$ (the relaxation function) and $\mu^{-1}(t)$ (the creep function), the governing equations are [4]; (See Fig. 1).

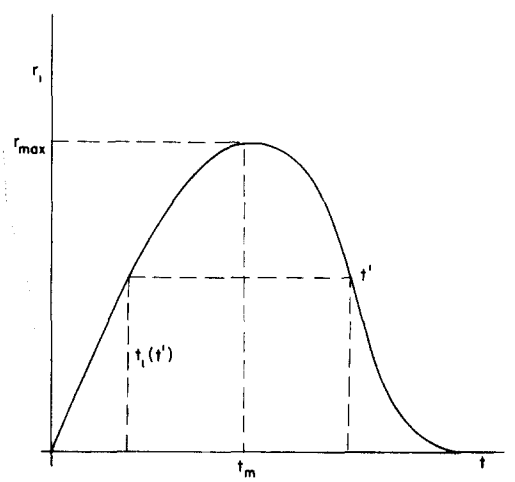

FIG. 1. Typical loading path for impact problem.

For $0 \leq t \leq t_m$

$$M\ddot{\alpha}(t) = -\frac{8R^{\frac{1}{2}}}{3(1-\nu)}\int_0^t \mu(t-t')\frac{\mathrm{d}}{\mathrm{d}t'}(\alpha^{\frac{3}{2}}(t'))\,\mathrm{d}t' \tag{1}$$

and

$$\alpha = r_1^2(t)/R \tag{2}$$

where ν is Poisson's ratio, and $r_1(t)$ is the current radius of contact.

For

$$t_m \leq t \tag{3}$$

$$R\alpha(t) = r_1^2(t) - \int_{t_m}^{t} \mu^{-1}(t-t')\frac{\mathrm{d}}{\mathrm{d}t'}\left[\int_{t_1(t')}^{t'} \mu(t'-t'')\frac{\mathrm{d}}{\mathrm{d}t''}(r_1^2(t''))\,\mathrm{d}t''\right]\mathrm{d}t'$$

and

$$M\ddot{\alpha}(t) = -\frac{8}{3R(1-\nu)}\int_0^{t_1(t)} \mu(t-t')\frac{\mathrm{d}}{\mathrm{d}t'}(r_1^3(t'))\,\mathrm{d}t' \tag{4}$$

We might note that for the loading case (i.e. α increasing) the relation between $\alpha(t)$ and $r_1(t)$ is identical with the elastic case. For unloading they differ (see Fig. 2) by the double integral involving the viscoelastic functions.

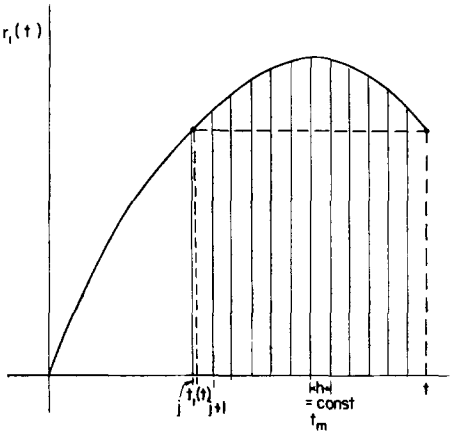

FIG. 2

If we take equation (1) and break up the integral into a finite number of integrals over small increments of time we obtain

$$M\ddot{\alpha}(t) = -\frac{8R^{\frac{1}{2}}}{3(1-\nu)}\sum_{i=1}^{N}\int_{t_i}^{t_{i+1}} \mu(t-t')\frac{\mathrm{d}}{\mathrm{d}t'}(\alpha^{\frac{3}{2}}(t'))\,\mathrm{d}t' \tag{5}$$

Since $\mu(t)$ is usually a smooth function we can approximate this expression by

$$M\ddot{\alpha}(t) \doteq -\frac{8R^{\frac{1}{2}}}{3(1-\nu)}\sum_{i=1}^{N}\tfrac{1}{2}[\mu(t-t_i)+\mu(t-t_{i+1})]\int_{t_i}^{t_{i+1}}\frac{\mathrm{d}}{\mathrm{d}t'}\alpha^{\frac{3}{2}}(t')\,\mathrm{d}t' \tag{6}$$

$$M\ddot{\alpha}(t) \doteq \frac{-8R^{\frac{1}{2}}}{3(1-\nu)}\sum_{i=1}^{N}\tfrac{1}{2}[\mu(t-t_i)+\mu(t-t_{i+1})][\alpha^{\frac{3}{2}}(t_{i+1})-\alpha^{\frac{3}{2}}(t_i)] \tag{7}$$

The most appropriate method to solve this equation appears to be a forward difference to obtain $\alpha(T+h)$, i.e.

$$\alpha(T+h) = \alpha(T)+h\dot{\alpha}(T)+\frac{h^2}{2!}\ddot{\alpha}(T) \tag{8}$$

Assume that α, $\dot{\alpha}$, $\ddot{\alpha}$ are known up to some time T. Then from equation (8) it is possible to calculate $\alpha(T+h)$. Equation (7) is then used to obtain $\ddot{\alpha}(T+h)$. From the following $\dot{\alpha}(T+h)$ is obtained

$$\dot{\alpha}(T+h) = \dot{\alpha}(T)+h\ddot{\alpha}(T) \tag{9}$$

The process is repeated to obtain $\alpha(T+2h)$, $\dot{\alpha}(T+2h)$ and $\ddot{\alpha}(T+2h)$.

Since the initial conditions are at $t = 0$, $\alpha = 0$, $\dot{\alpha} = V$, it is clear that the system is explicit if solved in the proper sequence.

From the solution of this system of equations one obtains the curve in Fig. 1 up to $t = t_m$. At this point $\dot{r} = 0$ and the calculation is stopped.

We now turn to equations (3) and (4) which are the governing system of equations.

Let

$$F(t') = \int_{t_1(t')}^{t'} \mu(t'-t'')\frac{\mathrm{d}}{\mathrm{d}t''}(r_1^2(t''))\,\mathrm{d}t'' \tag{10}$$

Then (3) becomes

$$R\alpha(t) = r_1^2(t)-\int_{t_m}^{t} \mu(t-t')\frac{\mathrm{d}F}{\mathrm{d}t'}(t')\,\mathrm{d}t'. \tag{11}$$

Assuming that $\mu(t)$ is smooth

$$R\alpha(t) \doteq r_1^2(t)-\sum_{i=1}^{M} \tfrac{1}{2}[\mu(t-t_i)+\mu(t-t_{i+1})][F(t_{i+1})-F(t_i)] \tag{12}$$

and using the same procedure as before

$$F(t') = \sum_{i=1}^{N} \tfrac{1}{2}[\mu(t'-t_i')+\mu(t'-t_{i+1}')][r_1^2(t_{i+1})-r_1^2(t_i')] \tag{13}$$

It is clear that since the function $F(t')$ depends on $t_1(t')$ [see definition of $F(t)$, equation (10)] which in turn is only known from the solution, that the system cannot be solved explicitly for the unknown functions. However a solution can be obtained by an iteration process which is described below.

If in equation (11) we take $\alpha(t_m+h)$ to be $\alpha(t_m+h) = \alpha(t_m)-\varepsilon$ then we can obtain $r_1(t_m+h)$ by an iteration. We know that $r(t_m+h) < r(t_m)$ for any finite h. Let

$$B = R\alpha(t_m+h)-r_1^2(t_m+h)+\int_{t_m}^{t_m+h} \mu(t-t')\frac{\mathrm{d}F(t')}{\mathrm{d}t'}\,\mathrm{d}t'.$$

By beginning the iteration with $r(t_m+h) = r(t_m)$ we know that we are above the value which makes $B = 0$. We slowly decrease r until B goes through zero.

The choice of $r(t_m+h)$ uniquely defines $t_1(t_m+h)$. To obtain the $F(t)$ integral we merely search through the table of solutions for $t < t_m$ to determine between what two r's the value of $r_1(t_m+h)$ lies. The integral to obtain $F(T)$ entails summing the products

$$F(T) = \sum_{i=1}^{N} \tfrac{1}{2}[\mu(T-t_i)+\mu(T-t_{i+1})][r_1^2(t_{i+1})-r_1^2(t_i)]$$

For $T = t_m+h$ there will be only two terms in this sum. In general there will only be one interval of non-standard width (see Fig. 2). In this figure we have shown what the picture looks like if calculations have been carried to some arbitrary point $t > t_m$.

The dependence of the solution on the choice of ε and h will be discussed in a later section.

NUMERICAL SOLUTIONS AND RESULTS

In order that there be some check on the solution of the integral equations, the ordinary differential equation describing the elastic impact problem was solved using a second order Euler method, i.e.

$$\alpha(T+h) = \alpha(T)+h\dot{\alpha}(T)+\frac{h^2}{2}\ddot{\alpha}(T)$$

$$M\ddot{\alpha}(T+h) = K\alpha^{\frac{3}{2}}(T+h) \qquad K = \text{material parameter}$$

where the initial conditions are $\alpha(0) = 0$, $\dot{\alpha}(0) = V$.

Then by making all the $G(t_i)$ and $J(t_i)$'s constant in the viscoelastic solution we were able to check that the solution obtained was the elastic solution.

Another point that is worth bringing out at this time is the restriction on the choice of mesh width.

Ordinarily in a solution to a system of equations of this type there is seldom a restriction on the minimum mesh that is used (other than a financial one). However in the region of decreasing $r_1(t)$, i.e. $t > t_m$ the solution entails taking the sum of two quantities which are opposite in sign and nearly equal in magnitude, i.e.

$$\int_{t_m}^{t} (t-t')\frac{dF}{dt'}dt' = \sum_{i=1}^{N} \tfrac{1}{2}[\mu(t-t_i)+\mu(t-t_{i+1})][F(t_{i+1})-F(t_i)].$$

Here $dF(t')/dt'$ is positive from $t_1(t')$ to t_m and negative from t_m to $t'(t' > t_m)$.

Hence when too small a mesh is used (in our case 1×10^{-6} sec) the sums may not be monotonic as they should be and the solution will not converge.

We now reopen the question of the dependence of the solution on the choice of ε [i.e. $\alpha(t_m+h) = \alpha(t_m)-\varepsilon$]. [In theory $\varepsilon = 0$ from equation (8)]. However it is better to choose it non-zero in order to start the calculation off smoothly. If ε is chosen to be considerably smaller than the value $\alpha(t_m)-\alpha(t_m-h)$ which is a reasonable restriction, the solution will converge to the "right" answer. (The same answer.) Another point where common sense must prevail is the manner in which $r_1(t)$ is decreased in the iteration process. If one insists on saving time by decreasing $r_1(t)$ in large steps then the solution will be crude to say the least. In our case we took δ (defined by $r_1(t_i) = r_1(t_{i-1})-\delta$) to be consistently

$\frac{1}{10}[r_1(t_{i-1})-r_1(t_{i-2})]$ with a starting value of

$$\delta = \tfrac{1}{10}[r_1(t_m)-r_1(t_m-h)].$$

The results of calculations made for temperatures ranging from 24°C to 128°C are shown below. In each case an elastic solution is shown for comparison. This solution is obtained using the same initial conditions and impacting sphere. The value of $G(t, T)$ at $t = 1 \times 10^{-6}$ sec and the appropriate temperature as well as a Poisson ratio of 0·3 are used as a material description for the elastic solutions.

In addition, the amount of error which is introduced by assuming that the relation $r_1 = \sqrt{(\alpha R)}$ holds for the unloading process is presented.

DISCUSSION OF NUMERICAL RESULTS

Before discussing the numerical results it is important to recall the assumptions and approximations that led up to these results, (in particular, the manner in which the constitutive relation was obtained). (See Appendix.) Then it will be possible to draw some general conclusions regarding the comparisons with the experimental results of [6].

The material description of the viscoelastic solid [i.e. $G(t)$, $J(t)$] was obtained from a series of free vibration experiments which produced for each temperature a value of $G_1(\omega)$ and $\tan\delta(\omega)$. These values were used together with an equation (see Kolsky [7]) which was based on the weak dependence of $\tan\delta$ on frequency to expand the range of values of $G(\omega)$. This frequency data was then converted through approximate formulae [see equations (14)–(18)] to obtain values of $G(t)$ and $J(t)$ from $t = 1$ μsec to 3000 μsec.

Even though we have as solutions to the integro-differential equation plots of $\alpha(t)$ and $r_1(t)$ from the beginning to end of the contact problem the only comparison with experiment that is possible is in the value of the total times of contact and the height to which the ball rebounds. Table 1 lists these comparisons.

As can be seen from Table 1, the agreement is quite good between the numerical solution and measured values both in time of contact and rebound height for the lower

TABLE 1. REBOUND DATA FOR AN $\frac{11}{16}$ IN. STEEL SPHERE DROPPING ONTO A BLOCK OF P.M.M.

(v_0 = 70·6 cm/sec)

T_0 (°C)	T_c measured (μsec)	T_c calculated (μsec)	h_r/h_0 % measured	h_r/h_0 % calculated
24		220		101
27	230		87	
45		224		83
47	231		86	
77		262		60
78*	257		77	
115		506		64
116	369		38	
128		652		55
129	463		24	
128 $r = \sqrt{(R\alpha)}$		736		41

temperatures. This is expected since it is at these temperatures that the inaccuracies of determining the input data are smallest. Correspondingly, it is at the lowest temperature that the numerical viscoelastic solution is closest to the elastic solution (which has been proven experimentally).

The curves which show the elastic as well as viscoelastic solution give some idea of the amount of error that one accepts when an elastic analysis is done on materials which are only slightly viscoelastic. However, it appears that the equivalent frequency concept [6] should be fairly useful for determining the dynamic modulus of P.M.M. up to say 55°C (depending, of course, upon how much error you are willing to accept). At this temperature the impact is still nearly Hertzian [8].

The fact that for room temperatures the rebound height was greater than 100 per cent reflects a small inaccuracy in the numerical scheme. However this was most apparent for the calculations at low temperatures where the curves are steepest. For the higher temperatures the error decreased as reflected in the elastic solutions. These results showed only about a 1 per cent error in the calculation of the rebound height. The error which occurred in the calculation of the time of contact was much less.

It should be pointed out that no optimum time interval was sought in determining any of these curves. The time interval that was used was one which worked reasonably well over all the temperatures at which we sought solutions and was thus used for convenience.

Some calculations were made to determine the sensitivity of the solution to the mesh width (Δt) and the choice of ε and δ. (See Fig. 9). There was only a slight change in the solution when we went from $\Delta t = 2 \times 10^{-6}$ sec to 1×10^{-6} sec, but the solution did not converge for $\Delta t < 1$ sec. For the dependence of the solution on ε and δ it was found that the difference was imperceptible if we decreased either by a factor of $\frac{1}{10}$. However this does not say that an *unreasonable* choice of either ε or δ would not result in serious error being introduced.

The solution shown in Fig. 12 sheds some light on the amount of error introduced by assuming that the relation $r = \sqrt{(R\alpha)}$ (Solution II) holds for the viscoelastic case. This is equivalent to forcing the material to stay in contact with the ball during withdrawal.

Here we see that for $T = 128°$ and relatively large damping (but not nearly as high as would occur closer to the transition region) that the two solutions differ considerably. How they compare depends upon the variables considered. It is clear that the maximum depth will be the same in either case. It appears that Solution II will always predict a longer time of contact and a lower rebound than I.

CONCLUSIONS

During the course of this investigation a complicated pair of nonlinear integro-differential equations involving hereditary functions have been solved. The solution was shown to be quite simple as numerical solutions go.

Considering the fact that in solving these equations only rough estimates of time of contact and height of rebound were sought, the data obtained in the vibration experiments and used to generate the material properties was adequate. For more accurate results much more attention must be paid to the material parameters used in the solution as well as the difference method and choice of mesh width.

In addition, the numerical solution of both the viscoelastic and elastic problems showed how the nature of the penetration changed as the temperature and hence the mechanical properties changed. These results shed some light on the limitation of the use of the equivalent frequency concept and consequently the limitation of using the ball bouncing method of dynamic testing.

Finally, for the case of $T = 128°C$, some quantitative information concerning the errors introduced by neglecting the difference between the areas of contact in the elastic and viscoelastic problems is presented.

Acknowledgements—The author is indebted to Professor H. Kolsky for many helpful discussions during the course of this investigation. He is also indebted to Mrs. P. Strauss for her assistance in programming the solution for the digital computer. Mr. L. Daubney and Mr. J. W. Phillips also assisted in the vibration experiments.

The financial support of the U.S. Army Research Office (Durham) and the Advanced Research Projects Agency under Contracts DA-31-124-ARO(D)358 and SD-86, respectively, is gratefully acknowledged.

REFERENCES

[1] T. C. T. TING, Brown University, Division of Engineering, Technical Report (1965).
[2] YOH-HAN PAO, *J. appl. Phys.* **26**, 1083 (1955).
[3] E. H. LEE and J. R. M. RADOK, *J. appl. Mech.* **27**, 438 (1960).
[4] S. C. HUNTER, *J. Mech. Phys. Solids* **8**, 219 (1960).
[5] G. A. C. GRAHAM, *Int. J. engng Sci.* (1966).
[6] H. H. CALVIT, Technical Report 1, ARO(D), Brown University, Division of Applied Mathematics (1966). (To be published in *J. Mech. Phys. Solids.*)
[7] H. KOLSKY, *Phil. Mag.* (1956).
[8] A. E. H. LOVE, *A Treatise on the Mathematical Theory of Elasticity*. Dover (1927).
[9] J. D. FERRY, *Viscoelastic Properties of Polymers*. Wiley (1961).

(*Received* 16 *January* 1967; *revised* 10 *April* 1967)

APPENDIX

Free Torsional Vibration of Rods of Polymethylmethacrylate (P.M.M.)

Vibration experiments were run on rods of P.M.M. to obtain the viscoelastic functions $\mu(t)$ and $\mu^{-1}(t)$ to be used in the numerical solutions previously discussed. Values of $G(\omega, T)$ were obtained for temperatures ranging from room temperature to 128°C. From these values of $G(\omega)$ using the methods outlined in Ferry [9] (and shown later) we were able to obtain values of $G(t)$ and $J(t)$ (these are the same as $\mu(t)$, $\mu^{-1}(t)$ presented in Hunter's article) to be used in the numerical solution of the rebound problem described earlier.

The specimens were rods 6 in. long and 2 in. and $\frac{1}{2}$ in. dia. For the larger diameter rod a circular plate of aluminum $\frac{3}{16}$ in. thick and 10 in. dia. was attached to one end. The other end of the rod was glued to the frame of the test jig. This combination of dimensions was chosen to produce high frequency response. (See Fig. 3.) The plate served as an inertial element as well as a means of introducing the forcing moments. These moments were created by putting alternating currents through the galvanometer type arrangement (see Fig. 4) attached on ends opposite of a diameter of the plate. A similar device was also used as a pickup to record the frequency and decay of the response.

It was important that the moments produced by the drivers were in the same sense and that they were oriented such as to produce as little flexure of the rod as possible. This

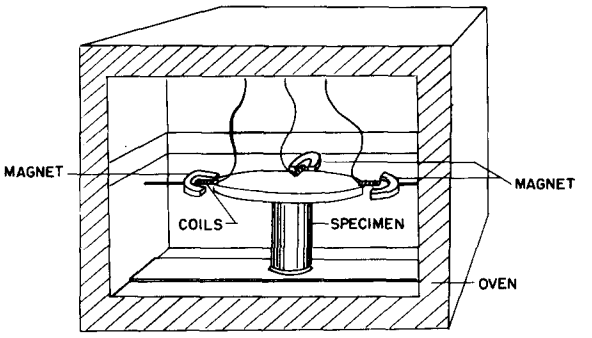

FIG. 3. Vibration test.

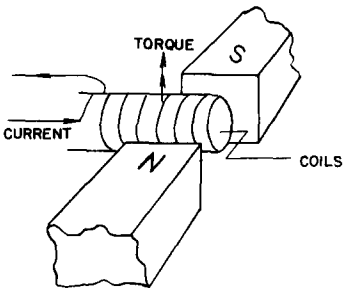

FIG. 4. Driving force arrangement.

became a more serious problem at the higher temperatures since the rigidity of the rod decreased enormously.

The output of the galvanometer pickup was fed into a dual beam C.R.O. and a picture was taken of the trace (see Fig. 5). The signal was also fed into a digital counter which measured and displayed the frequency of the response. The top trace shows the decay of the motion after the external forces have been discontinued and the bottom, the forcing signal from the oscillator.

From the photograph (Fig. 5) we are able to obtain the frequency of the free vibration and its logarithm decrement. By knowing the inertia of the system it is possible to obtain $G(\omega)$ from the frequency. From the value of the logarithmic decrement $\tan\delta$ is obtained. (See Ferry [9].)

$$G_1(\omega) = (\omega_c^2 I/b)(1+\Delta^2/4\pi^2) \tag{14}$$

$$G_2(\omega) = (\omega_c^2 M/b)\Delta/\pi \tag{15}$$

$$\tan\delta = G_2/G_1$$

where Δ = logarithmic decrement; I = moment of inertia of disk; ω_c = resonant frequency; b = form factor

$$G_1(\omega) = G_{1c}\left(1+\frac{2\tan\delta}{\pi}\ln\frac{\omega}{\omega_c}\right) \tag{16}$$

$$G(t) = G_1(\omega) - 0{\cdot}40G_2(0{\cdot}4\omega) + 0{\cdot}014G_2(10\omega) \tag{17}$$

where $\omega = 1/t$ and G_{1c} is the value of G_1 at $\omega = \omega_c$.

$$J(t) = \sin M\pi/M\pi G(t) \tag{18}$$

where M is the slope of the doubly logarithmic plot of $G(t)$.

These calculations then produce the necessary functions to be used in calculating $\alpha(t)$ and $r_1(t)$ for the impact problem.

Experimental Results

The data obtained from the 2 in. dia. bar are shown at the end of the paper.

Figure 5 is an oscilloscope trace showing the manner in which the free vibration decayed with time.

The logarithmic decrement was obtained by measuring the amplitude of successive maxima and taking the logarithm of the ratios, i.e.

$$\Delta = \ln \frac{x_i}{x_{i+1}}$$

This was computed for several successive cycles and an average computed and recorded for this temperature. Figure 7 shows a plot of Δ vs. temperature and Fig. 8, tan δ vs. temperature. (The relative maximum at about 80° is attributed to the response of the Tra-Con cement which was used to stick the specimen to the frame.) Also $G_1(\omega)$ vs. temperature is shown in Fig. 6.

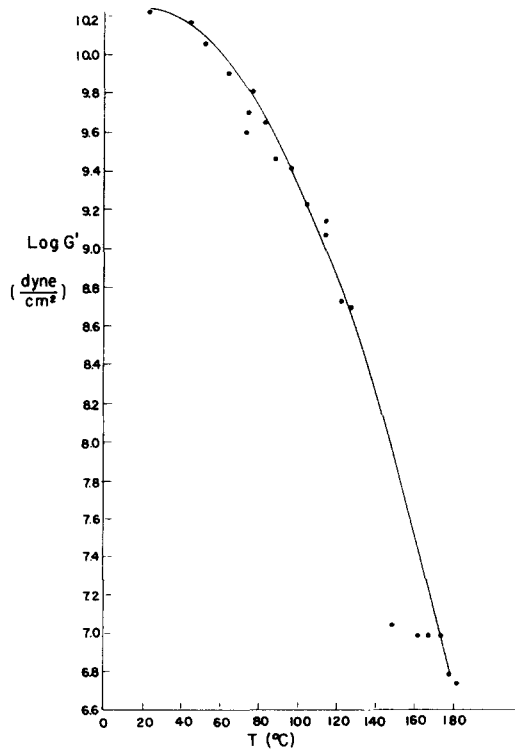

FIG. 6

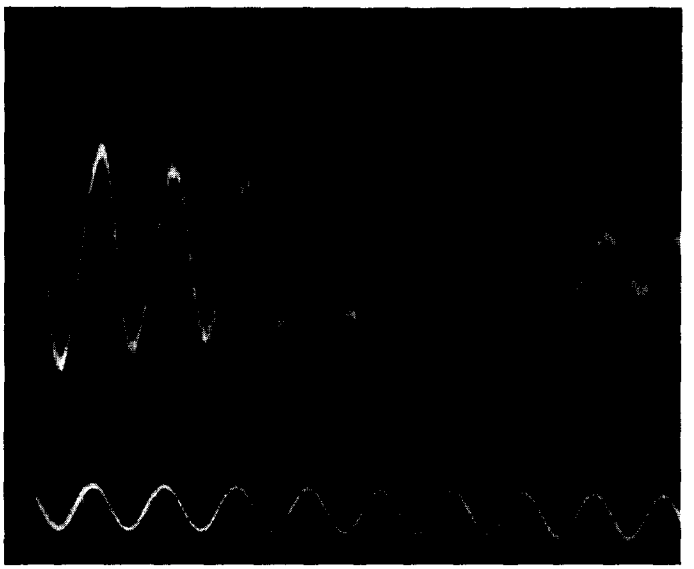

FIG. 5

[*facing page* 960

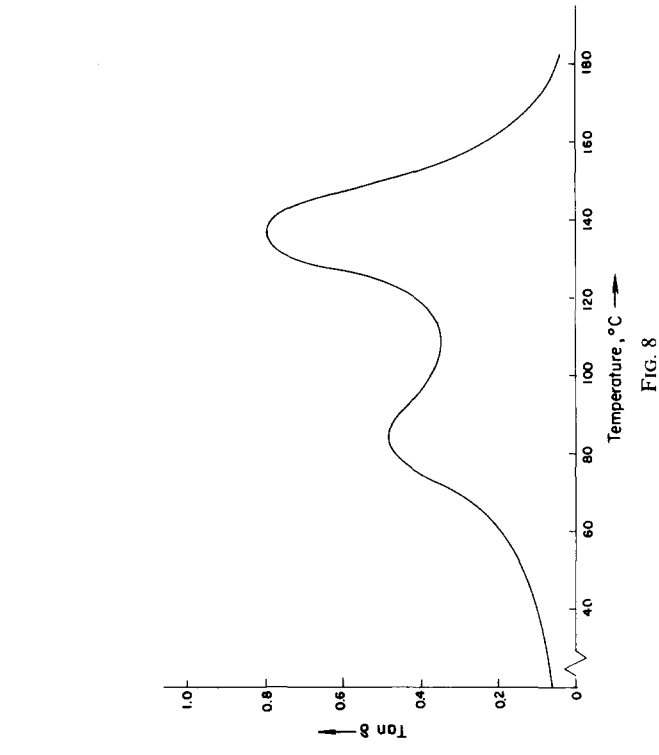
Tan δ
0
0.2
0.4
0.6
0.8
1.0
40
60
80
100
120
140
160
180
Temperature, °C

FIG. 8

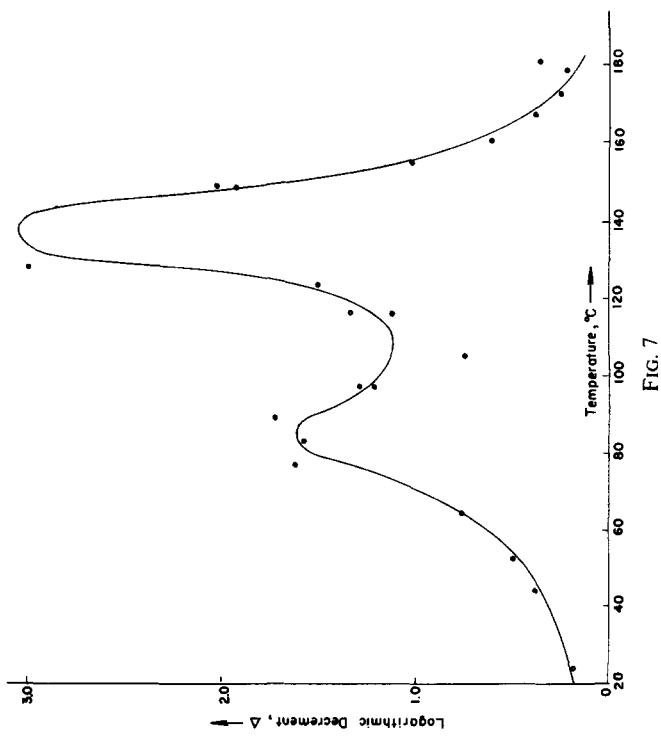
Logarithmic Decrement, Δ
0
1.0
2.0
3.0
20
40
60
80
100
120
140
160
180
Temperature, °C

FIG. 7

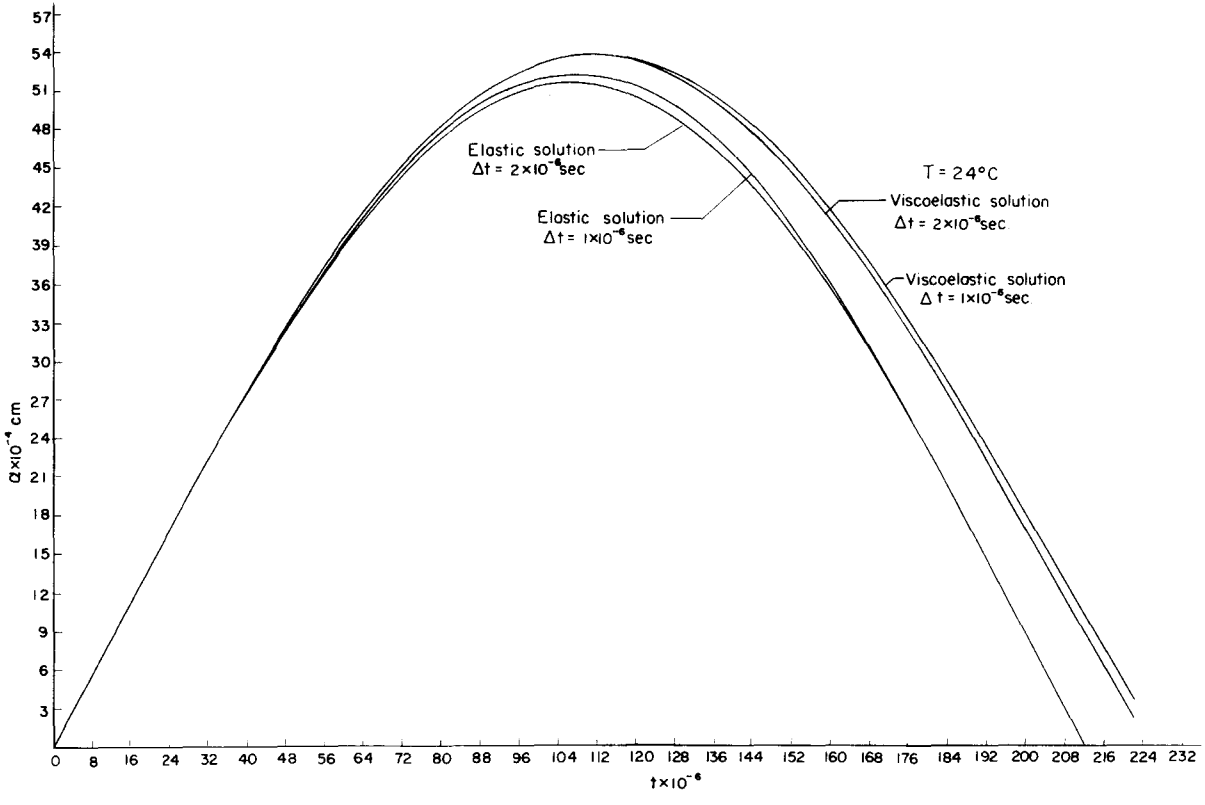
Elastic solution
Δt = 2×10⁻⁶sec
Elastic solution
Δt = 1×10⁻⁶sec
T = 24°C
Viscoelastic solution
Δt = 2×10⁻⁶sec
Viscoelastic solution
Δt = 1×10⁻⁶sec
a×10⁻⁴ cm
t×10⁻⁶
57
54
51
48
45
42
39
36
33
30
27
24
21
18
15
12
9
6
3
0 8 16 24 32 40 48 56 64 72 80 88 96 104 112 120 128 136 144 152 160 168 176 184 192 200 208 216 224 232

FIG. 9

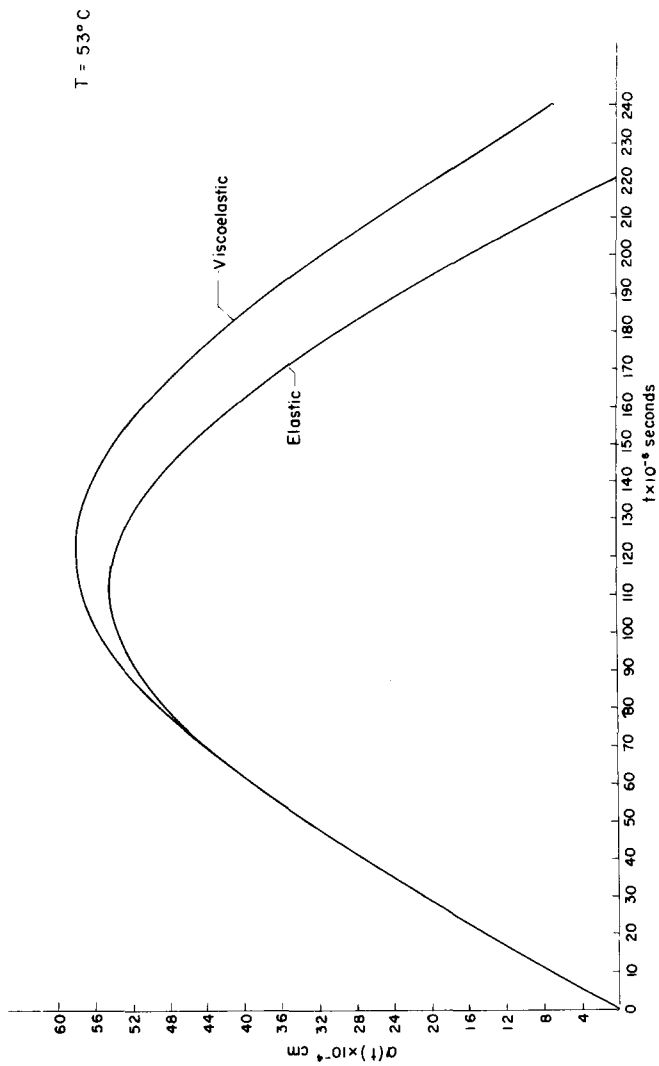
T = 53° C
Viscoelastic
Elastic
σ(t)×10⁻⁴ cm
t×10⁻⁶ seconds
0
10
20
30
40
50
60
70
80
90
100
110
120
130
140
150
160
170
180
190
200
210
220
230
240
4
8
12
16
20
24
28
32
36
40
44
48
52
56
60

FIG. 10

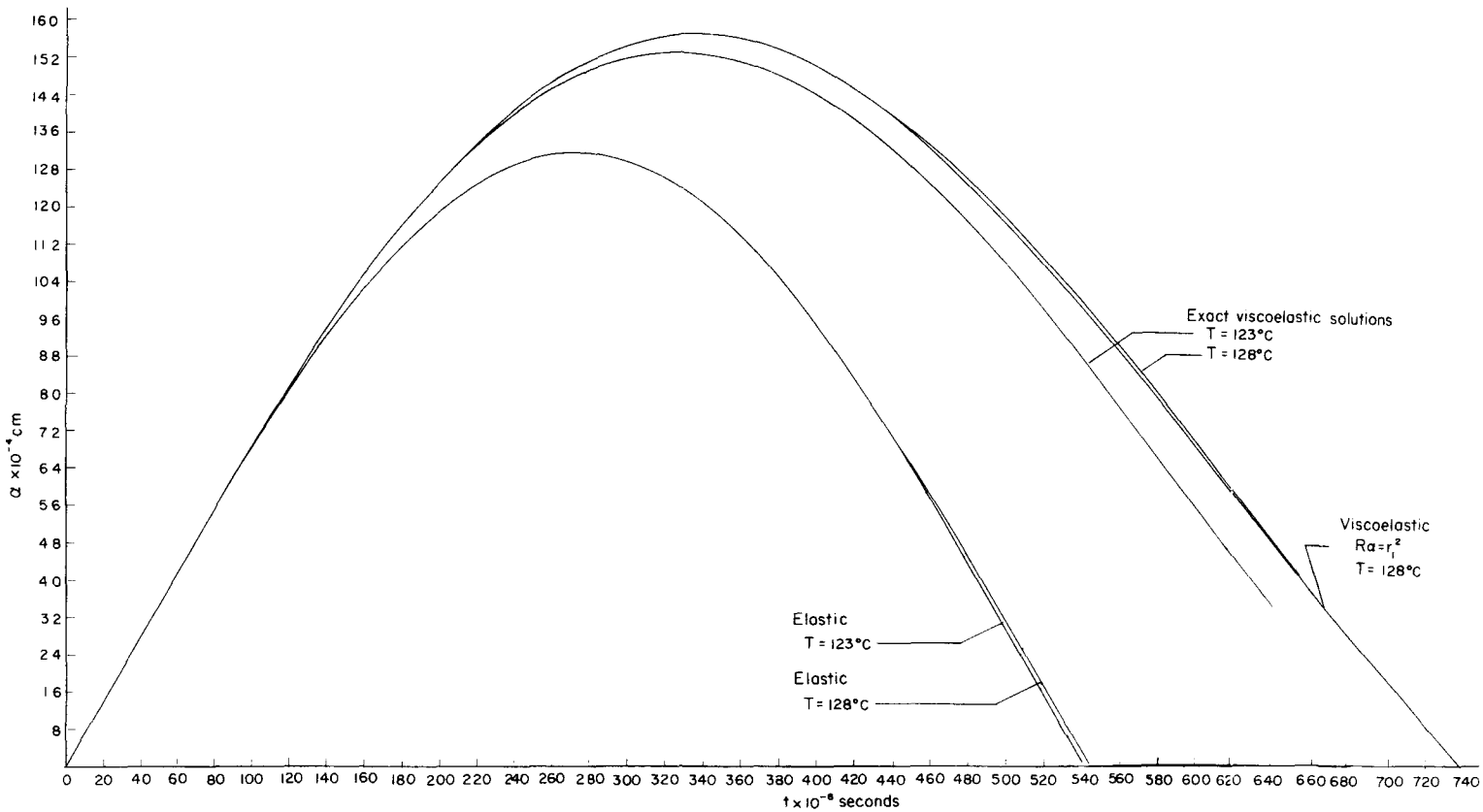
160
152
144
136
128
120
112
104
96
88
80
72
64
56
48
40
32
24
16
8
α x10⁻⁴cm
0 20 40 60 80 100 120 140 160 180 200 220 240 260 280 300 320 340 360 380 400 420 440 460 480 500 520 540 560 580 600 620 640 660 680 700 720 740
t x10⁻⁶ seconds
Exact viscoelastic solutions
T = 123°C
T = 128°C
Viscoelastic
Rα=r₁²
T= 128°C
Elastic
T = 123°C
Elastic
T= 128°C

FIG. 11

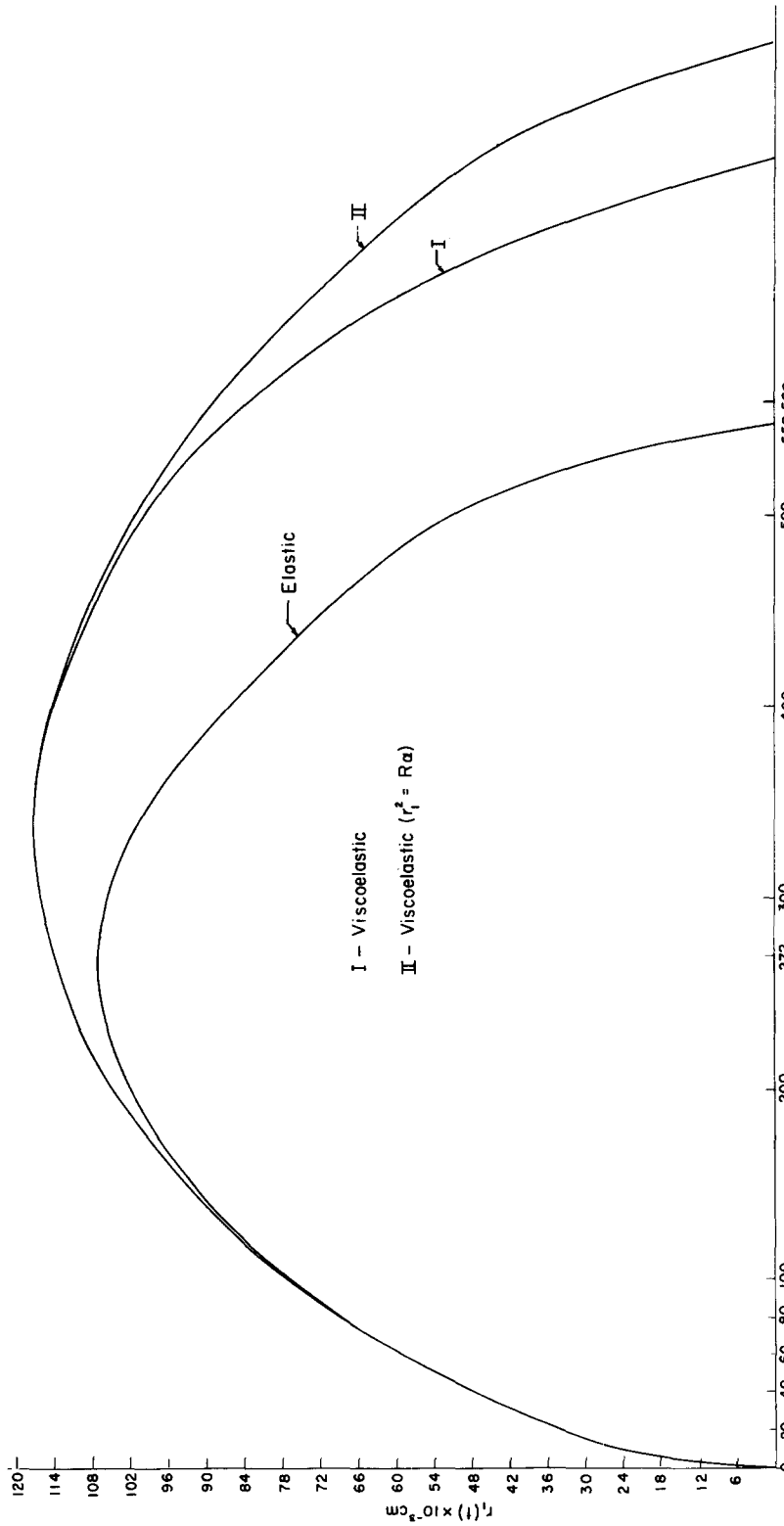
Elastic
I – Viscoelastic
II – Viscoelastic ($r_1^2 = Ra$)
I
II
$r_1(t) \times 10^{-3}$ cm
$t \times 10^{-6}$ seconds
0 20 40 60 80 100 200 272 300 400 500 550 560
6 12 18 24 30 36 42 48 54 60 66 72 78 84 90 96 102 108 114 120

FIG. 12

Discussion of the Data

Since the data from the larger diameter bar appeared best, only these results were presented. There were a number of problems which developed in testing the small diameter specimen which made the results suspect. In particular the large mass attached to the top of the specimen had to be supported by a bead type chain of very low torsional rigidity. However at higher temperatures the bar itself had almost no rigidity and thus the question of the effect of the chain was raised. Also due to lack of rigidity, there were other problems of flexure of the specimen, wind resistance, etc. However there was fairly good agreement at the lower temperatures (less than 110°C) which gave us confidence in the data for the 2 in. rod.

It should also be pointed out that it is not correct to use the formulae (14, 15) for calculating values of $\tan \delta$ from the decrement for large values of $\tan \delta$ (or Δ). Thus for an accurate measure of damping one must concentrate on the values of Δ which were obtained from experiment.

Résumé—La paire d'équations intégro-différentielles non linéaires couplées qui décrivent la résilience d'une sphère rigide par rapport à une masse semi-infinie viscoélastique sont résolues numériquement. En faisant usage de données obtenues à partir d'expériences de vibration de torsion libre, le rebondissement d'une balle en acier sur un bloc de polymère est prédit pour différentes températures. Ces résultats sont comparés à des expériences de rebondissement effectuées sur le même matériau. La solution viscoélastique est aussi comparée à des solutions élastiques et à une solution approximative. Quelques conclusions sont tirées sur l'usage de la méthode de rebondissement comme moyen d'essais dynamiques.

Zusammenfassung—Das gekoppelte Integral-Differential-Gleichungspaar, das den Stoss einer starren Kugel gegen einen viskoelastischen Halbraum beschreibt, wird numerisch gelöst. Indem Daten verwendet werden, die bei Versuchen mit freien Drehschwingungen erhalten wurden, wird die Rückprallhöhe einer Stahlkugel von einem Polymärblock für verschiedene Temperaturen vorausgesagt. Diese Resultate werden mit Versuchsergebnissen verglichen die mit den gleichen Materialien gemacht wurden. Ferner wird die viskoelastiche Lösung mit der elastischen Lösung und mit der Annäherungslösung verglichen. Gewisse Schlüsse werden gezogen über die Verwendung der Rückprallmethode zur dynamischen Messung.

Абстракт—Дается численный расчет сопряженной лары нелинейных интегрально-дифференциальных уравнений, которые описывают удар твердого марика в вязкоупругое полупространство. Используя результаты полученные из экспериментов для свободных крутильных колебаний иредсказывается отражение стального шарика от блока полимера при разных температурах. Зти результаты сравниваются с экспериментами на отражение приведенными для этого же самого материала. Далее, сравнивается вязко-упругое решение с упругим решением, а также с приближенным решением. В заключении даются некоторые выводы, которые разрешают использование метода отражения в смысле динамического опыта.